

Chemistry and Biology of Macrolide Antiparasitic Agents

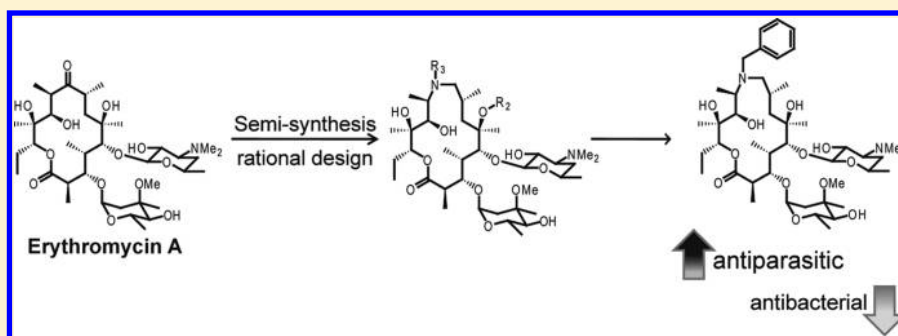
Younjoo Lee,[†] Jun Yong Choi,^{||} Hong Fu,[†] Colin Harvey,[†] Sandeep Ravindran,[‡] William R. Roush,^{||} John C. Boothroyd,[‡] and Chaitan Khosla^{*,†,§}

[†]Department of Chemistry, [‡]Department of Microbiology and Immunology, and [§]Department of Chemical Engineering, Stanford University, Stanford, California 94305, United States

^{||}Department of Chemistry, Scripps Florida, Jupiter, Florida 33458, United States

S Supporting Information

ABSTRACT:



Macrolide antibacterial agents inhibit parasite proliferation by targeting the apicoplast ribosome. Motivated by the long-term goal of identifying antiparasitic macrolides that lack antibacterial activity, we have systematically analyzed the structure–activity relationships among erythromycin analogues and have also investigated the mechanism of action of selected compounds. Two lead compounds, *N*-benzylazithromycin (11) and *N*-phenylpropylazithromycin (30), were identified with significantly higher antiparasitic activity and lower antibacterial activity than erythromycin or azithromycin. Molecular modeling based on the cocrystal structure of azithromycin bound to the bacterial ribosome suggested that a substituent at the N-9 position of desmethylazithromycin could improve selectivity because of species-specific interactions with the ribosomal L22 protein. Like other macrolides, these lead compounds display a strong “delayed death phenotype”; however, their early effects on *T. gondii* replication are more pronounced.

INTRODUCTION

Apicomplexan parasites such as *Plasmodium falciparum* and *Toxoplasma gondii* are ubiquitous human pathogens. Malaria, caused by *Plasmodium* spp., is responsible for more than one million deaths per year, primarily in children, whereas *T. gondii*, the etiologic agent of toxoplasmosis, causes serious morbidity and mortality in pregnant women and immunocompromised individuals undergoing chemotherapy or with AIDS.^{1–3} There is considerable interest in developing safer drugs against these protozoan infections, ones that are appropriate for therapy or prophylaxis in infants and pregnant women. At the same time, emerging resistance toward existing chemotherapeutic agents is also prompting the search for new antiparasitic drugs.

Apicomplexan parasites harbor a plastid (bacterial-like) organelle called the apicoplast that is recognized as a particularly attractive drug target.⁴ Small molecules that prevent protein biosynthesis on the plastid ribosome show antiparasitic activity. For example, tetracyclines such as doxycycline, which bind to the 30S subunit in bacterial ribosome, are commonly used as antimalarial prophylactic agents^{5–7} (even though doxycycline is contraindicated during pregnancy and in children less than 8

years of age). Similarly, antibiotics that target the 50S subunit such as lincosamides, chloramphenicol, and macrolides also display moderate antiparasitic activities.⁸ All of these compounds show a characteristic “delayed death phenotype”, presumably because of their ability to induce a time-dependent reduction in the copy number of the apicoplast genome.⁴

Macrolide antibiotics such as erythromycin are widely used to treat respiratory tract infections caused by Gram-positive bacteria. Although laboratory and clinical studies have demonstrated that azithromycin, a semisynthetic erythromycin analogue, has some efficacy against *Toxoplasma*⁹ and *Plasmodium*,^{10–12} macrolides have not yet found extensive use as antiparasitic agents, presumably because of suboptimal efficacy and concerns regarding the potential emergence of resistance against this frontline antibacterial agent. Identification of a parasite-specific macrolide with higher potency than erythromycin or azithromycin would therefore represent a significant advance in the field of parasitology. Because of the stability of azithromycin in the acidic gastric

Received: December 15, 2010

Published: March 23, 2011

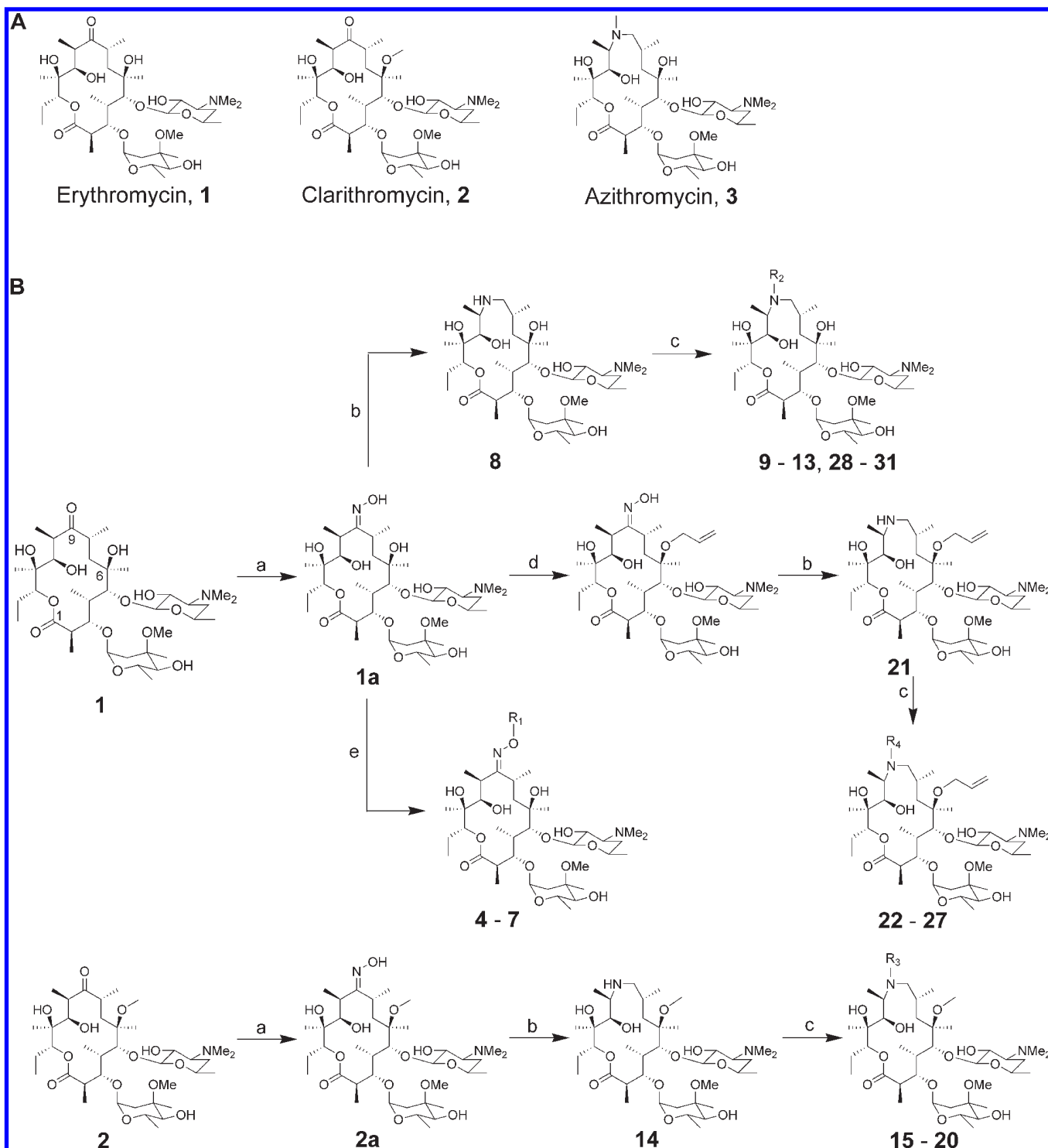


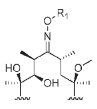

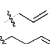
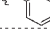
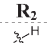
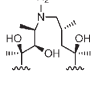
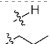
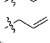
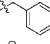
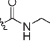
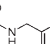
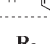
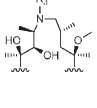
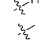
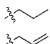
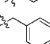
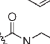
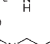
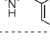
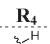
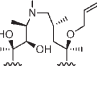
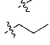
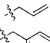
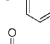
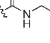
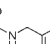
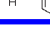

Figure 1. (A) Structures of erythromycin, clarithromycin, and azithromycin. (B) Synthesis of erythromycin A oxime ethers (**4–7**) and 15-membered azithromycin analogues (**8–31**): (a) 50% NH_2OH (aq), AcOH in isopropanol; (b) (i) toluene-*p*-sulfonyl chloride in MeOH, (ii) NaBH_4 in MeOH; (c) corresponding aldehyde, AcOH, NaBH_3CN in DMF; (d) (i) pyridine·HCl, cyclohexane diethyl ketal in CH_3CN , (ii) pyridine·HCl, hexamethyldisilazane in CH_3CN , (iii) allyl *tert*-butylcarbonate, $\text{Pd}_2(\text{dba})_3$, dppb in THF, (iv) AcOH in CH_3CN and H_2O ; (e) corresponding alkyl halides, 1 M potassium *tert*-butoxide in THF.

environment, its high serum half-life and tissue penetration, and its well-documented safety profile in children and pregnant women,^{13–15} this semisynthetic macrolide was identified as a particularly attractive starting point for our investigations. Our studies were significantly aided by the recently solved

high-resolution crystal structures of prototypical bacterial 50S ribosomes in complex with a number of macrolide antibiotics.^{16–24}

The structures of azithromycin bound to the 50S ribosomal subunit from the eubacterium *Deinococcus radiodurans* (DS0S)²²

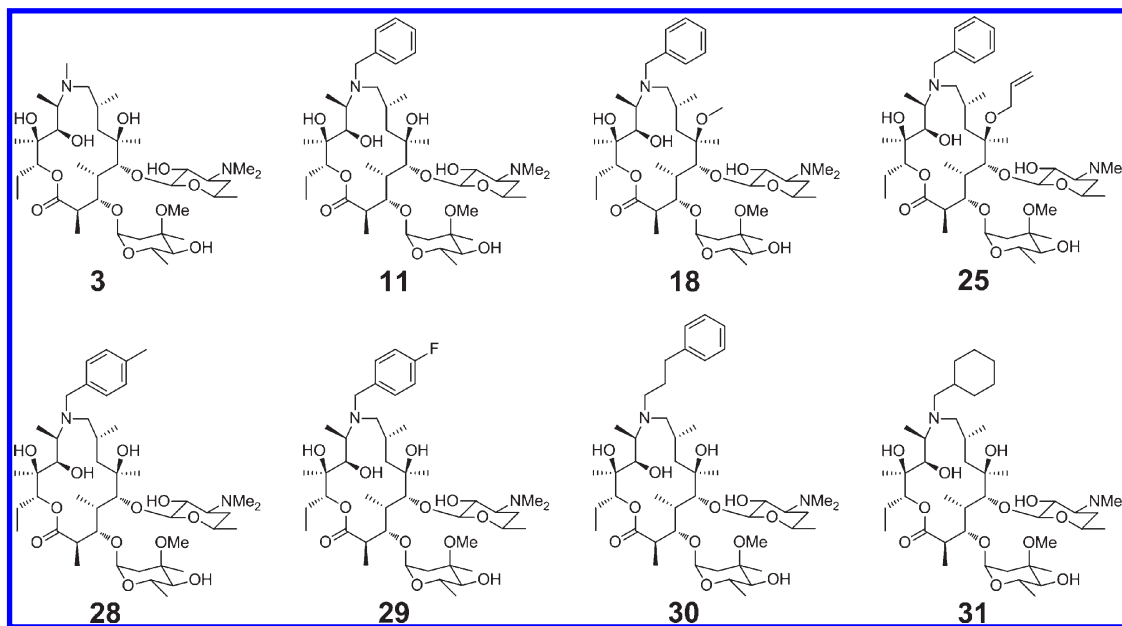
Table 1. Antiparasitic, Antibacterial, and Cytotoxic Activities of Semisynthetic Erythromycin Analogues^a

Compd. #		IC ₅₀ (μM) <i>T. gondii</i>	MIC (μM) <i>B. subtilis</i>	CC ₅₀ (μM)	
1	Erythromycin	93 ± 10	0.04	475	
2	Clarithromycin	31 ± 5	0.04	260	
3	Azithromycin	20 ± 2	0.15	174	
R₁					
	4		14 ± 2	0.04	22
	5		1.6 ± 0.2	0.04	7
	6		2.7 ± 1	0.04	16
	7		1.4 ± 0.1	0.04	3
R₂					
	8		65 ± 7	1.2	386
	9		16 ± 3	0.6	139
	10		13 ± 2	0.3	103
	11		2 ± 0.2	0.3	32
	12		85 ± 3	10	480
	13		12 ± 0.3	1.2	222
R₃					
	14		106 ± 11	2.5	460
	15		89 ± 7	5	454
	16		20 ± 2	1.2	106
	17		13 ± 1	0.8	84
	18		2 ± 0.1	0.3	13
	19		59 ± 4	10	409
	20		16 ± 0.4	1.5	62
	R₄				
	21		40 ± 1	2.5	74
	22		25 ± 0.7	10	96
	23		15 ± 0.6	10	42
	24		12 ± 0.4	5	38
	25		5 ± 0.3	6	14
	26		33 ± 2	5	90
	27		6 ± 0.4	1.5	28

^a To quantify the antiparasitic activity of each compound, cultures of human foreskin fibroblast (HFF) cells grown in 96-well plates were infected with *T. gondii* 2F-1 YFP₂ (*T. gondii* YFP)³⁶ expressing the yellow fluorescent protein under control of a constitutive promoter. Each compound was titrated into infected cultures at varying dilutions. Infected cultures were incubated for 4 days (two infection cycles) in the continuous presence of compounds. Antibacterial activity was measured as the minimum inhibitory concentration (MIC) against the representative Gram-positive bacterium *B. subtilis*. Two-fold incremental dilutions of each compound were added to freshly inoculated cultures of *B. subtilis*. The lowest concentration at which no growth was observed was recorded as the MIC. Cytotoxicity was determined in parallel with antibacterial and antiparasitic activity with MTS (3-(4,5-dimethylthiazol-2-yl)-5-(3-carboxymethoxyphenyl)-2H-tetrazolium) assay. Low passage HFF cells (2×10^3 cells/well) were seeded into the 96-well culture plates and incubated for 24 h at 37 °C. Then the HFF cells were exposed to the various concentrations of macrolides for 2 days. After incubation, the macrolide treated medium was aspirated, and fresh medium and MTS were added in order. The plates were incubated for 4 h at 37 °C, and the optical density was measured at 490 nm. CC₅₀ was determined by cytotoxic dose of macrolides reducing cell viability by 50%.

and to that of the archaeon *Haloarcula marismortui* (H50S)²³ have been solved. In D50S, two azithromycin molecules bind cooperatively to the tunnel. The macrolactone ring (through hydrophobic interactions) and the desosamine sugar (through hydrogen bonding) of the first azithromycin (AZ-1) interact with the minor groove edges of nucleotides A2058Ec and A2059Ec of domain V of the 23S RNA subunit (Ec = *E. coli* numbering). The binding mode of AZ-1 is in accordance with that of the entire

macrolide antibiotic family. The second molecule (AZ-2) reaches domain II of the 23S RNA and also engages ribosomal proteins L4 and L22 through hydrophobic interactions. Together, the two molecules effectively block the exit tunnel of the ribosome. In H50S, G2058Ec (instead of A) hinders the binding of one azithromycin molecule and displaces the remaining macrolactone ring toward the tunnel wall. This residue is representative of eukaryotic rRNA sequences. As a result of this displacement,

Table 2. Antiparasitic, Antibacterial, and Cytotoxic Activities of Selected Azalides^c

compd	IC ₅₀ (μM)				MIC ^a (μM)	CC ₅₀ ^b (μM)
	0 h		6 h			
	first cycle	second cycle	first cycle	second cycle		
3	29 ± 2	0.6 ± 0.07	44 ± 5	0.6 ± 0.03	0.15	174
11	5 ± 1	0.5 ± 0.10	9 ± 1	0.5 ± 0.05	0.3	32
18	7 ± 0.3	5 ± 0.2	10 ± 1	4 ± 0.5	0.3	13
25	7 ± 1	10 ± 1	>10	>10	6.0	14
28	5 ± 1	0.6 ± 0.04	9 ± 1	0.7 ± 0.05	0.3	38
29	6 ± 1	0.5 ± 0.07	9 ± 1	0.7 ± 0.01	0.3	31
30	4 ± 1	0.6 ± 0.06	8 ± 1	0.6 ± 0.01	0.6	33
31	7 ± 1	0.6 ± 0.10	12 ± 2	0.6 ± 0.07	0.3	36

^a MIC: minimum inhibitory concentration against *B. subtilis*. ^b CC₅₀: cytotoxic concentration at which human foreskin fibroblast viability drops by 50%. ^c “0 h” data refer to results from experiments in which macrolide and parasite were simultaneously added to fibroblast cultures, whereas “6 h” data were obtained from experiments in which parasites were first allowed to infect before addition of the macrolide.

azithromycin partially blocks the exit tunnel of the archeon ribosome, consistent with its lower binding affinity to this target. Thus, in principle, azithromycin can achieve species selectivity as a result of subtle differences between the structures of prokaryotic and eukaryotic ribosomes.²⁵ We sought to exploit these differences in our design of an antiparasitic macrolide. Specifically, multiple sequence alignment revealed high sequence identity in domain V residues of the *T. gondii* and *B. subtilis* 23S RNA that are likely to interact with azithromycin (Table S1 in Supporting Information). However, domain II and the ribosomal proteins L4 and L22 are less conserved in regions that are presumably relevant to macrolide binding. We therefore prepared and evaluated a set of erythromycin analogues that (a) have the potential of interacting with domain II, L4, and/or L22 and (b) are unlikely to be prohibitively expensive to synthesize on a large scale.

RESULTS

Synthesis of Erythromycin and Azithromycin Analogues. Modifications at the C-9 ketone of erythromycin or the N-9 amine of azithromycin are relatively easy to introduce and are likely to point toward L4 and L22. Alkylation at the C-6 position also has precedence (as in the case of clarithromycin) and is known to introduce beneficial conformational changes to the macrolide ring and to afford interactions with domain II.^{22,26,27}

To modify the C-9 position of erythromycin, we synthesized a series of erythromycin oxime ether analogues modeled after the antibacterial agent roxithromycin.^{28,29} The N-9 position of azithromycin was modified by varying alkyl or arylalkyl substituents on the nitrogen atom. Both classes of compounds included analogues with unmodified or alkylated 6-OH groups.

The synthesis of erythromycin oxime ethers and azithromycin analogues followed earlier synthetic precedents (Figure 1B).^{29–34} Briefly, 9(*E*)-erythromycin A-oxime (**1a**) was quantitatively obtained from erythromycin A by treatment with hydroxylamine in

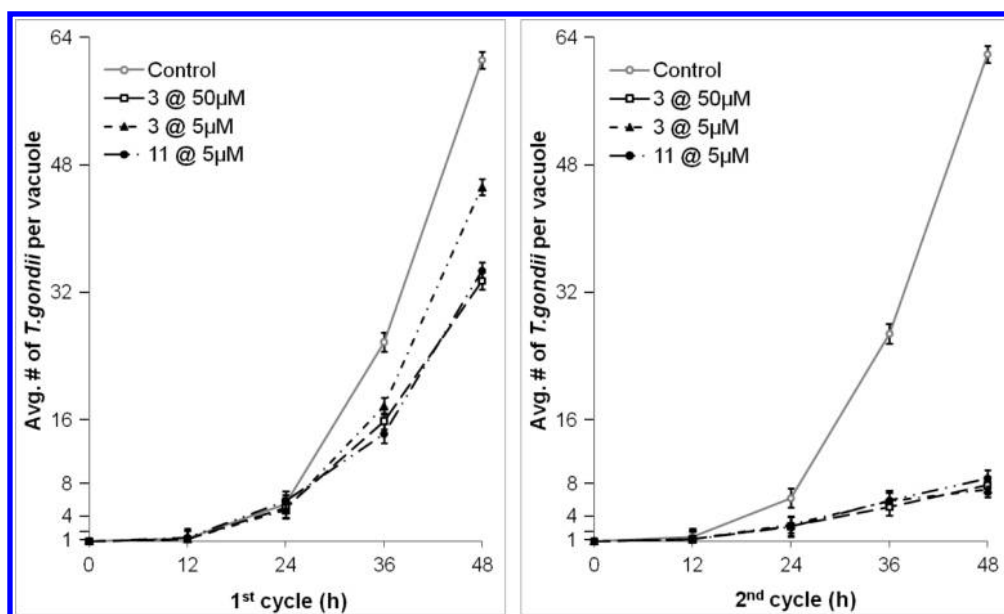


Figure 2. Effect of azithromycin (**3**) and **11** on cell division of *T. gondii*. The number of GFP parasites per parasitophorous vacuoles was scored at 12 h intervals, assuming that each vacuole starts with a single *T. gondii* cell. Each data point is an average of three independent experiments. Average parasite counts were obtained by counting at least 50 randomly selected vacuoles in each well. Only the data for cultures exposed to antibiotics at 0 h are shown. The data for cultures in which drug was added at 6 h were similar and are therefore not shown.

the presence of acetic acid. The synthesis of erythromycin A 9-oxime ethers (**4**–**7**) was accomplished in a single step by treating oxime **1a** with corresponding alkyl halides and potassium *tert*-butoxide.

For the synthesis of azithromycin analogues, 9(*E*)-erythromycin A-oxime (**1a**) was activated with sulfonyl chlorides for the Beckmann rearrangement, thus converting a ring-expanded imino ether compound. Subsequent reduction afforded a 15-membered aza-macrolide, often referred to as an azalide. Azithromycin (**3**) was obtained by methylating this secondary amine at the 9a position, whereas other azalides were obtained via reductive amination with aldehydes and cyanoborohydride.³⁵

Biological Activities of Erythromycin Analogues. As an initial test of the biological activities of our erythromycin analogues, we measured their antiparasitic, antibacterial, and cytotoxic activities (Table 1). Half-maximal inhibitory concentrations (IC₅₀) were measured in a parasite growth assay using an engineered strain of *Toxoplasma gondii* 2F-1 YFP₂.³⁶ Parasite growth was monitored over the course of 4 days. Separately, the minimum inhibitory concentrations (MIC) of each compound against a representative Gram-positive bacterium *Bacillus subtilis* were measured in standard 2-fold dilution assays. Last, the half-maximal cytotoxic concentration (CC₅₀) of each compound was measured using uninfected human fibroblast cultures as the test system. On the basis of these results, two of the most promising compounds (**11** and **18**) were azithromycin analogues in which the ring nitrogen was alkylated with a benzyl substituent. Compared to azithromycin, they had markedly improved antiparasitic activity and reduced antibacterial activity. Oxime ethers, including compounds **5** and **7**, also had good antiparasitic activity, although they retained strong antibacterial activity. The antibacterial activity of azalides drops when the ring nitrogen harbors a substituent other than a methyl group^{37–39} or when the 6-OH group is alkylated or both.

Differential Effects of Alternative Azalides on *T. gondii*. Macrolides are known to exhibit peculiar kinetics with respect to

their antiparasitic activity, a phenomenon that is sometimes referred to as the “delayed death phenotype”.^{4,40,41} For example, azithromycin is a weak inhibitor of parasite replication during the first cycle of fibroblast infection (IC₅₀ = 29 µM; Table 2). However, the resulting parasites are severely compromised in their ability to replicate in a second fibroblast infection cycle, even when the second infection cycle is performed in the absence of any antibiotic. Indeed, exposure of *T. gondii* to less than 1 µM azithromycin in the first cycle results in a >2-fold reduction in parasite titers by the end of the second infection cycle (Table 2). Using azithromycin as a control, we therefore quantified the effects of compounds **11**, **18**, and **25** on parasite proliferation in each of two successive infection cycles (Table 2). By using two slightly different protocols in these experiments, we were also able to investigate the effect of each compound on the biology of extracellular versus intracellular *T. gondii*. In one protocol, fibroblasts were infected with *T. gondii* YFP cells in the presence of individual macrolides. The infected cultures were then incubated for 48 h (first cycle). Thereafter, the parasites released by lysed fibroblasts were harvested and inoculated into fresh fibroblast cultures (second cycle). No macrolide antibiotic was added to the second cycle cultures. In an alternative protocol, *T. gondii* YFP cells were first allowed to infect the host fibroblast cells for 6 h. Thereafter, the fibroblasts were washed to remove parasites that had not invaded the host cells and replenished with fresh media containing macrolides. After 42 h (i.e., at the end of the first cycle), the released parasites were harvested as before and used to inoculate fresh fibroblast cultures for a second cycle, again without supplementary macrolide. In both protocols, the IC₅₀ values of compound **11** were markedly higher after the first cycle than the second cycle, whereas neither compound **18** nor **25** showed this delayed death phenotype. These observations suggested that, whereas compound **11** is genuinely a more potent analogue of azithromycin, the observed antiparasitic activities of compounds **18** and **25** may result from a different mode of

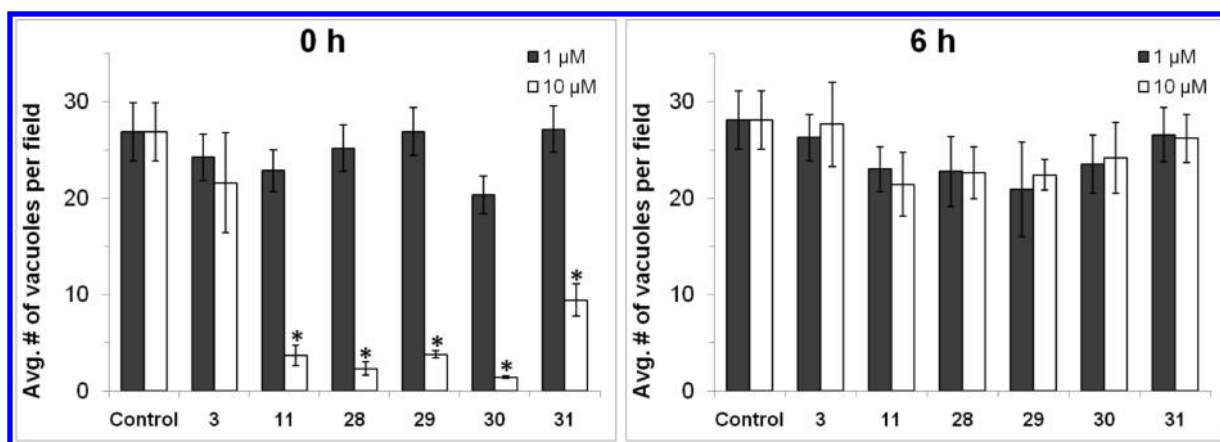


Figure 3. Effect of macrolides on *T. gondii* infectivity. The number of vacuoles per microscope field was scored 24 h into the first infection cycle. At least 20 randomly selected microscope fields from each of three experiments were scored to obtain each data point. For the treatment of compounds 11 and 28–31 at the 0 h procedure, differences between 1 and 10 μM were highly significant (*, $p < 0.001$).

action. We therefore focused our attention on the preparation and evaluation of additional analogues of 11.

Structure–Activity Relationship (SAR) Analysis of Compound 11. On the basis of the above data, we designed a focused set of N-9 substituted arylazalides. Our primary goal was to explore whether subtle steric or electronic changes in the N-9 substituent could affect antiparasitic activity. Representative analogues with electron donation into (28) or withdrawal from (29) the benzyl ring were targeted. We also sought to examine whether improved activity could result from increasing the flexibility of the linker to the aromatic ring (30). In addition, the need for an aromatic group at this position was tested by preparing and assaying cyclohexyl analogue 31.

To prepare these analogues, intermediate 8 was reacted with the corresponding aldehydes, and the resulting Schiff's bases were reduced as before. The macrolides were assayed as above, using azithromycin and 11 as controls. In addition, their MIC values against *B. subtilis* and cytotoxicity toward uninfected human foreskin fibroblasts (calculated as CC_{50}) were also measured. The overall in vitro pharmacological profiles of these compounds are summarized in Table 2. Compound 31 has slightly higher IC_{50} values compared to other benzylated compounds 28–30 at the first infectious cycles. Whereas the second cycle antiparasitic activities of compounds 11 and 28–31 are similar to azithromycin, the new analogues have substantially better growth inhibitory activity than azithromycin in the first infection cycle. The bulkier substituent at the N9 position in the macrocyclic ring also conferred a modest increase in mammalian cell cytotoxicity, although the therapeutic index ($\text{CC}_{50}/\text{IC}_{50}$) remained unchanged owing to improved growth inhibition in the first cycle. One of the new analogues (30) showed a further reduction in antibacterial activity, which may mitigate potentially deleterious effects on commensal microflora in animal studies involving chronic dosing. The lowest dose of azithromycin that significantly protects mice against death due to acute toxoplasmosis is 200 (mg/kg)/day.⁵⁰ Thus, compounds 11 and 28–31 could potentially be administered at lower doses because of increased antiparasitic activities. In all cases the therapeutic index appears to be adequately high for experimental animal use compared to azithromycin and clarithromycin.

Further Investigations into the Mode of Action of Selected Azalides. Several additional experiments were performed

to understand better the mechanism of delayed death of apicomplexan parasites that are treated with macrolide antibiotics. First, we monitored parasite replication noninvasively over the course of the first and second infectious cycles using *T. gondii* $\text{RH}\Delta\text{hwgprt}$ GFP. This strain expresses the green fluorescent protein and can therefore be visualized and counted in individual parasitophorous vacuoles of infected fibroblasts. In the first infection cycle, fibroblasts infected with *T. gondii* were exposed to azithromycin (5 or 50 μM) or analogue 11 (5 μM). Both infection protocols described earlier (i.e., drug addition at 0 and 6 h) were used. In these infection protocols, a small but measurable inhibitory effect was observed in the first cycle, whereas much stronger inhibition of *T. gondii* replication was observed in the second cycle (Figure 2). Consistent with the population-averaged IC_{50} values reported in Table 2, compound 11 was more active than azithromycin in the first infection cycle, whereas both macrolides had comparable activities in the second cycle. Intracellular *T. gondii* parasites divided approximately every 8 h (or shorter, given that parasites that had already lysed out of the host cell were not counted). In contrast, when parasites were treated with azithromycin (50 μM) or 5 μM compound 11, the doubling time increased to ~ 9.5 h in the first infection cycle. At all concentrations tested in the second infection cycle, parasite doubling times had increased to >16 h. Thus, it appears that the antiparasitic activity of macrolides is, at least in part, due to their ability to inhibit the replication rates of protozoan parasites inside mammalian cells.

We also sought to test whether macrolides reduced the frequency of successful infections in the first infection cycle or not. The density of parasitophorous vacuoles was estimated at 24 h postinfection, using both the “0 h” and “6 h” infection protocols described above. Azithromycin and compounds 11 and 28–31 were tested in parallel experiments. As seen in Figure 3, at 10 μM , azalides 11 and 28–31 (but not azithromycin) show a marked decrease in the density of parasitophorous vacuoles but only when added concurrently with the parasite inoculum (i.e., at 0 h). Vacuole density remains unaffected by all macrolides in pre-infected fibroblasts (i.e., when the antibiotic is added at 6 h). Together, these findings demonstrate that the new macrolides reported here are able to attenuate the infectivity of extracellular *T. gondii* even in the first infection cycle. Thus, their overall antiparasitic effects are presumably the cumulative result of two modes of actions.

Table 3. Copy Number Ratios of Apicoplast/Nuclear Genome in Response to Antibiotic Treatment^a

		first cycle (48 h)		second cycle (48 h)	
		<i>T. gondii</i> RHΔ	<i>T. gondii</i> Clin ^R -4	<i>T. gondii</i> RHΔ	<i>T. gondii</i> Clin ^R -4
control		20 ± 3	26 ± 4	21 ± 3	21 ± 5
3	10 μM	10 ± 2	10 ± 3	3 ± 1	4 ± 1
	1 μM	7 ± 1	8 ± 3	3 ± 1	3 ± 1
	0.1 μM	7 ± 4	18 ± 2	15 ± 5	13 ± 4
11	10 μM	13 ± 3	11 ± 2	6 ± 2	5 ± 1
	1 μM	7 ± 2	8 ± 1	5 ± 1	3 ± 0.3
	0.1 μM	13 ± 5	23 ± 2	17 ± 7	15 ± 4
clindamycin	1 μM	6 ± 1 ^b	12 ± 2 ^b	3 ± 1 ^b	9 ± 1 ^b
spiramycin	5 μM	8 ± 3	8 ± 1	5 ± 0.4	3 ± 0.2
pyrimethamine	1 μM	29 ± 8	27 ± 2	22 ± 2	23 ± 4

^a Control, azithromycin (3), compound 11, and reference compounds (clindamycin, spiramycin, and pyrimethamine) were evaluated via real-time quantitative PCR assay (RT-PCR). The copy numbers were determined based on the ratio of two genes synthesized from primer sets of a plastid gene (*ycf24*, Genbank accession U87145) and a nuclear gene (*UPRT*, U10246). *T. gondii* RHΔ*hxgprt* and *T. gondii* Clin^R-4⁴⁴ were allowed to infect a monolayer of HFF cells. After 6 h, the medium was changed, and the parasites were incubated for 42 h in the presence of different concentrations of compounds. At 48 h after infection, parasites (*T. gondii* RHΔ*hxgprt* and *T. gondii* Clin^R-4⁴⁴) were isolated and reinoculated into the fresh HFF monolayer and incubated for 48 h in the absence of compounds. ^b Statistical analysis (by the *t* test) indicates that the genome ratios in clindamycin-treated *T. gondii* RHΔ*hxgprt* are distinct from those of clindamycin-treated *T. gondii* Clin^R-4 in both cycles ($p < 0.001$).

Macrolides Induce a Comparable Loss of Apicoplast DNA in Clindamycin-Sensitive and Clindamycin-Resistant *T. gondii*. We sought to verify that the new macrolides described in this report were indeed inhibitors of apicoplast replication. In these experiments, we also chose to evaluate other clinically relevant ribosome inhibitors, such as the 16-membered macrolide spiramycin and chloramphenicol and the lincosamide clindamycin.^{8,40,41} All these antibiotics show the delayed death phenotype. Pyrimethamine, an antiparasitic antibiotic that inhibits nuclear DNA replication,⁴² was used as a negative control.

Intracellular parasites ("6 h" infection protocol) were treated with varying concentrations (0.1, 1, and 10 μM) of azithromycin (3), 11, 25, or 30, as well as 1 μM clindamycin and 5 μM spiramycin throughout the first infection cycle. After 42 h, extracellular parasites released from the first cycle were reinoculated into fresh HFF cell monolayers in the absence of additional antibiotics. Real-time polymerase chain reaction (RT-PCR) was used to quantify the copy number ratio of the apicoplast genome versus nuclear genome; a single-copy nuclear gene (*UPRT*) and a single-copy plastid genome (*ycf24*) were targeted for amplification.⁴³

As seen in Table 3, pyrimethamine did not affect the ratio of plastid to nuclear DNA in either infection cycle. Also, as predicted from the data in Table 2, the apicoplast copy number was only marginally affected upon addition of compound 25, confirming that its antiparasitic activity was likely due to a distinct mode of action. In contrast, apicoplast replication in *T. gondii* RHΔ*hxgprt* was significantly impaired in even the first infection cycle in the presence of azithromycin, compounds 11 and 30, clindamycin, and spiramycin. In each case, further decrease in apicoplast copy number was observed in the second infection cycle. Dose dependence was also observed in each case.

We also sought to determine whether the clindamycin-resistant *T. gondii* Clin^R-4 strain⁴⁴ was resistant to azithromycin or compound 11. Both growth inhibition assays and quantitative RT-PCR assays were performed using the "0 h" and "6 h" infection protocols described above. Because *T. gondii* Clin^R-4 lacked the YFP transgene, parasite cells were counted with a

hemocytometer under the microscope. At both 1 and 10 μM, neither azithromycin nor compound 11 showed a noticeable difference between the wild-type and mutant *T. gondii* strains (data not shown). A similar conclusion was also obtained when the apicoplast/nuclear DNA ratio was quantified in the presence of macrolides 3 (azithromycin), 11, and spiramycin (Table 3). Thus, it appears that drug resistance of the *T. gondii* Clin^R-4 strain is specific for the lincosamides. This mutant possesses a 1857-(Ec) G → U point mutation in the apicoplast 50S rRNA, a site that is known to influence peptide translation.⁴⁴ In contrast, macrolides block the exit tunnel of the 50S subunits of both wild-type and mutant ribosomes.

Homology Modeling of the Apicoplast and Bacterial Ribosomes with Bound Macrolides. Because the crystal structures of ribosomes from *T. gondii* and *B. subtilis* were unavailable, a molecular modeling approach was used to analyze potential binding interactions between these ribosomes and the N-9 amine substituent of azithromycin. Multiple sequence alignments of the 50S rRNA and the L4 and L22 proteins were performed, and homology models of the target rRNAs were generated based on the published structure of *D. radiodurans* rRNA^{22,50} using the MOE program (Molecular Operating Environment, Chemical Computing Group Inc., Montreal, Canada). These homology models included two molecules of 11, parts of the rRNA near the azithromycin binding site, and the complete L4 and L22 proteins. Models were minimized using the Amber99 force field to remove any steric clashes. In the *T. gondii* rRNA model (Figure 4B), the phenyl ring of Phe98 was positioned ~6 Å from the phenyl ring of 11-2. The model also suggested that the adenine ring of A1441Tg was close to the phenyl ring of 11-2. In contrast, in the *B. subtilis* model, the equivalent amino acid was Pro87, located ~9 Å from the N-phenyl moiety of 11-2 (Figure 4C).

DISCUSSION

Although its function is still unclear, the apicoplast has received much attention as an attractive target for new drugs against apicomplexan parasites such as *Plasmodium* spp. and *Toxoplasma gondii*.⁴ Macrolide antibacterial agents bind to the

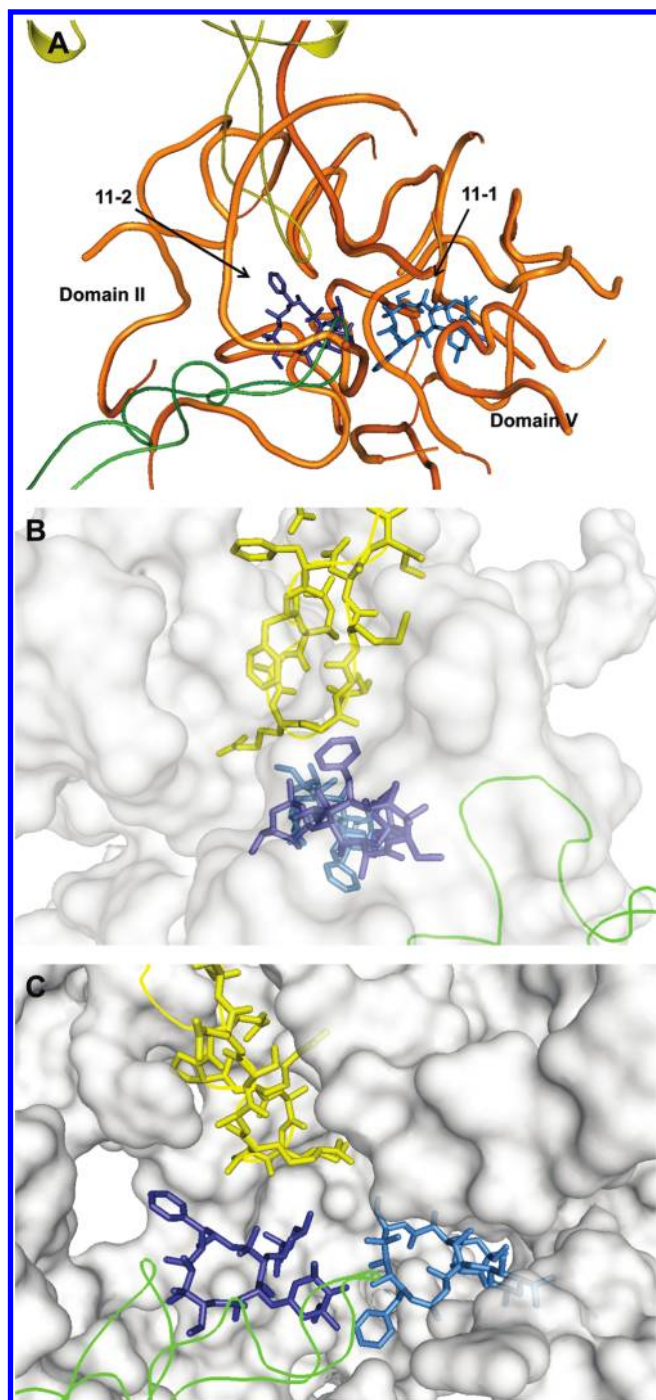


Figure 4. Homology models of the macrolide binding region of *D. radiodurans* (A), *T. gondii* (B), and *B. subtilis* (C) ribosomes, each with two copies of compound **11** (designated **11-1** and **11-2**). Because two azithromycin molecules are bound to the cocrystal structure of the *D. radiodurans* ribosome, two molecules of **11** (**11-1** and **11-2**) were used in the generation of our homology models. Structures **11-1** and **11-2** are light blue and dark blue, respectively. RNA fragments are shown as orange tubes or gray surfaces, and L4 and L22 proteins are in green and yellow, respectively. Pymol, version 1.0, was used to generate the figures. For details, see text.

large (50S) ribosomal subunit of the protozoan apicomplast and thereby also exhibit antiparasitic activity. Through the systematic design, synthesis, and biological characterization of a series of

erythromycin analogues, we not only have established prototypical structure–activity relationships but have also identified two promising azithromycin analogues with markedly higher antiparasitic activity and lower antibacterial activity than clinically available macrolides. In addition to providing potentially valuable new probes for investigating apicomplast biology in vivo, these compounds demonstrate the feasibility of engineering ribosome-binding antibiotics that are capable of discriminating between prokaryotic and selected eukaryotic pathogens.

Among the clinically available macrolides tested, azithromycin proved to be the best starting point for new antiparasitic agent discovery. The other macrolides (erythromycin, clarithromycin, and roxithromycin) predominantly rely upon hydrogen bonds and hydrophobic contacts with the 23S rRNA in the peptidyl transferase cavity to achieve their antibiotic activities.²¹ Although contacts between these macrolides and ribosomal proteins have not been structurally observed,²¹ there is certainly scope for such interactions due to conformational changes in the flexible L22 hairpin at the exit tunnel.^{27,45} Indeed, mutations in ribosomal proteins L4 and L22 that result in resistance toward erythromycin or other macrolides have been identified in several bacterial strains.^{46–49} In contrast, azithromycin appears to inhibit protein translation by a markedly different mechanism. In the crystal structure of *Deinococcus radiodurans* (D50S),²² two molecules of azithromycin bind in a perpendicular orientation to block the protein exit tunnel. The molecule that binds in the nonconserved mode interacts with ribosomal proteins L4 and L22. We speculate that the maintenance of this 2:1 macrolide/ribosome stoichiometric ratio contributes significantly to the improved antiparasitic activity of azalides such as **11** and **30**. Preservation of the hydrogen bond between the 6-OH of these azalides and C2565 in domain V of the 23S rRNA is critical for this atypical stoichiometry. At the same time, we hypothesize that the presence of an aromatic substituent at N-9 improves species selectivity because of potential interactions with ribosomal proteins L4 and/or L22 in *T. gondii*, which may differ in degree with those in *B. subtilis* (Table S1). The increased bulkiness of the N-9 substituent in compound **30** relative to **11** may enhance selectivity by reducing its affinity for the bacterial ribosome. Together, these results provide a starting point for a more intensive SAR investigation with the goal of maximizing antiparasitic activity in a macrolide that concomitantly lacks physiologically significant antibacterial activity.

Homology models of the *T. gondii* and *B. subtilis* rRNAs were generated based on the structure of the *D. radiodurans* rRNA (Figure 4A).^{22,50} These homology models included two molecules of **11**, parts of the rRNA near the azithromycin binding site, and the complete L4 and L22 proteins. These models suggested that, whereas the *N*-phenyl moiety of **11-2** could not favorably interact with *B. subtilis* L22, favorable edge-to-face interactions with Phe98 in the *T. gondii* L22 were possible. It is noted that the estimated distance between the two phenyl rings is larger than the optimal distance for an edge-to-face aromatic interaction (~ 3.7 Å).⁵¹ Energy minimization alone is presumably insufficient to define the optimal arrangement of these aromatic functional groups.⁵² Favorable interactions may require the L22 loop region (Phe97 to Arg108) to be dynamic.⁵³

Perhaps most importantly, three interesting conclusions can be drawn from our biological studies on azithromycin and its analogues. First, notwithstanding the well-documented delayed death phenotype of apicomplast inhibitors, compounds such as **11** and **30** induce rapid changes in *T. gondii* parasites. At low

micromolar concentrations, they attenuate both apicoplast copy number (Table 3) and parasite growth rates (Table 2) within the first infection cycle. Thus, it appears that, even though defective apicoplasts exert their most overt effects in secondary cycles of infection, the biology of the protozoan cell starts to be altered on a much shorter time scale. Second, azalides affect both the infectivity of apicomplexan parasites in mammalian cells (Figure 3) and the kinetics of cell division in the resulting parasitophorous vacuoles (Figure 2). It is tempting to assume that both these features result from inhibition of the apicoplast ribosome, although this remains to be established. If not, then *in vivo* studies in animals will be required to establish which of these mechanisms is more critical to the observed antiparasitic activity of azalides. This in turn would guide the judicious selection of a primary assay for more intensive SAR efforts. Last but not least, the reason for the low but measurable cytotoxic activity of azalides against human fibroblasts (Table 2) needs to be better understood. Several investigators have demonstrated toxicity of azithromycin against cultured mammalian cells at concentrations in the 100 μM range.^{54–56} The precise mechanism for these cytotoxic effects is unknown. However, a closely related macrolide antibiotic megalomicin is known to inhibit intra-Golgi trafficking⁵⁷ and lysosomal function⁵⁸ at comparable concentrations. Deconvolution of the structural features of azalides that contribute to mammalian cell toxicity from those that enhance binding to the apicoplast ribosome could greatly enhance the chance of discovery of a new antiparasitic macrolide with a suitable safety profile for eventual clinical use.

EXPERIMENTAL PROCEDURES

Materials. Antibiotics used were purchased from TCI America (Boston, MA) or Sigma-Aldrich (Milwaukee, WI). Solvents and chemical reagents were from Fisher Scientific, Inc. (Springfield, NJ) or Sigma-Aldrich. Reactions were carried out under an N_2 atmosphere in oven-dried glassware unless otherwise specified. Moisture- and oxygen-sensitive reagents were handled in an N_2 -filled drybox. The synthesis of erythromycin oxime ethers and azithromycin analogues followed earlier synthetic precedents.

General Methods. Analytical thin layer chromatography (TLC) was performed on precoated silica gel plates (60F₂₅₄) and flash chromatography on silica gel (230–400 mesh). TLC spots were detected by UV and/or by staining with a water-based cerium molybdate stain. Inova 400, Inova 500, and Inova 600 MHz NMR spectrometers were used to perform ¹H and ¹³C NMR analysis, and spectra were recorded in CDCl_3 . ¹H and ¹³C NMR spectra are reported as chemical shift in parts per million (multiplicity, coupling constant in Hz, integration). All final compounds were further introduced to liquid chromatography–mass spectrometry (LC–MS, Waters 2795 HPLC system) on a reverse phase C₈ column (2.1 mm \times 40 mm). Linear gradient elution was performed at 0.2 mL/min with CH_3CN and H_2O (both containing formic acid, 0.1%). The purity of each compound was calculated from the LC chromatogram at a wavelength of 210 nm. By this method, the purity of each compound was greater than or equal to 95.0%.

The procedures detailed below for compounds **4**, **9**, **10** and **12** are representative of the procedure followed for synthesis of all of the erythromycin A 9-oxime ethers and azithromycin analogues. Erythromycin A 9-oxime (**1a**) and intermediates **8**, **14**, and **21** were prepared as described. Scale, yield, and spectra are presented for each of the individual antibiotics assayed.

Erythromycin A 9-Oxime, 1a. Erythromycin A (0.68 mmol, 0.5 g) was dissolved in isopropanol (1.2 mL). Then 50% hydroxylamine (aq)

(620 μL) and acetic acid (190 μL) were added to the reaction mixture, and the mixture was stirred for 15 h at 50 °C. After the reaction mixture was allowed to cool to room temperature (rt), the reaction was quenched by saturated NaHCO_3 (aq). The isopropanol was removed under rotovap, and chloroform was added to extract the product. The chloroform extract was washed with brine, and the product was vacuum-dried and used for the following reactions without further purification.

Erythromycin A 9-Oxime Methyl Ether, 4. Erythromycin A 9-oxime **1a** (0.27 μmol , 200 mg) was dissolved in 1:1 mixture of THF and DMF (2 mL). 1-Iodomethane (0.32 μmol , 46 mg) and 1 M potassium *tert*-butoxide in THF (0.30 μmol , 300 μL) were added to the reaction mixture at 0 °C under N_2 . The mixture was stirred for 30 min at 0 °C and further stirred for 2.5 h at rt under N_2 . The crude mixture was diluted into CH_2Cl_2 and was washed three times with saturated NaHCO_3 (aq) and was dried over Na_2SO_4 . After evaporation of the solvent, the resulting product was purified by flash chromatography, eluting with a step gradient ranging from 3% to 10% $\text{MeOH}/\text{CH}_2\text{Cl}_2$ containing 0.1% NH_4OH (aq) to yield **4** (23.4 mg, 12%) as a white powder. ¹H NMR (500 MHz, CDCl_3) δ 5.10 (dd, $J = 11.1, 2.2$ Hz, 1H), 4.91 (d, $J = 4.7$ Hz, 1H), 4.47–4.37 (m, 2H), 4.04 (dd, $J = 9.6, 1.3$ Hz, 1H), 4.03–3.99 (m, 1H), 3.81 (s, 3H), 3.70–3.63 (m, 2H), 3.57 (d, $J = 7.5$ Hz, 1H), 3.48 (tdd, $J = 11.4, 6.6, 4.7$ Hz, 1H), 3.31 (s, 3H), 3.21 (dd, $J = 10.3, 7.3$ Hz, 1H), 3.11 (s, 1H), 3.02 (s, 1H), 2.90 (dq, $J = 14.3, 7.0$ Hz, 1H), 2.65 (q, $J = 7.0$ Hz, 1H), 2.42 (ddd, $J = 12.3, 10.4, 3.9$ Hz, 1H), 2.36 (d, $J = 15.1$ Hz, 1H), 2.28 (s, 6H), 2.25–2.19 (m, 1H), 2.18–2.15 (m, 1H), 2.02–1.95 (m, 1H), 1.91 (tdd, $J = 15.2, 8.7, 6.4$ Hz, 2H), 1.79 (s, 1H), 1.64 (ddd, $J = 24.0, 8.2, 5.6$ Hz, 2H), 1.59–1.52 (m, 2H), 1.50–1.43 (m, 1H), 1.46 (s, 3H), 1.30 (d, $J = 6.2$ Hz, 3H), 1.23 (s, 3H), 1.22 (d, $J = 6.1$ Hz, 3H), 1.18 (d, $J = 5.4$ Hz, 3H), 1.16 (d, $J = 5.4$ Hz, 3H), 1.12 (s, 3H), 1.10 (d, $J = 7.5$ Hz, 3H), 1.02 (d, $J = 7.0$ Hz, 3H), 0.83 (t, $J = 7.4$ Hz, 3H). ¹³C NMR (500 MHz, CDCl_3) δ 175.41, 171.71, 103.08, 96.40, 83.19, 79.99, 78.13, 77.75, 77.09, 75.48, 74.37, 72.82, 71.08, 70.64, 68.96, 65.65, 61.91, 49.62, 44.81, 40.41, 39.17, 37.90, 35.16, 32.97, 28.75, 27.17, 26.49, 21.63, 21.56, 21.21, 18.78, 18.74, 16.35, 16.27, 14.61, 10.83, 9.30. ESI mass spectrum: calcd (MH^+) 763.5; found 763.5.

9-Deoxy-9a-aza-9a-homoerythromycin A, 8. Erythromycin A 9-oxime (0.67 mmol, 0.5 g) dissolved in methanol (2.5 mL) was cooled to 5 °C, and toluene-*p*-sulfonyl chloride (0.80 mmol, 153 mg) was added to the reaction mixture followed by water. While the mixture was stirred for 5 h at 5 °C, pH of the reaction was maintained at 6–7 by adding 20% NaOH (aq). The crude mixture was diluted into water, adjusted to pH 6 with 1 N HCl, and extracted with methylene chloride twice. After adjustment of the pH to 8 with 20% NaOH (aq), extraction with methylene chloride was performed to yield erythromycin A imino ether. Erythromycin A imino ether (0.27 mmol, 0.2 g) dissolved in methanol (5 mL) was cooled to 4 °C, and sodium borohydride (5.4 mmol, 204 mg) was added in portions. The mixture was stirred for 36 h at rt. Dry ice was added to the reaction mixture until precipitation was completed, and the precipitate was filtered off. The filtrate was concentrated, and redissolved in chloroform. To the mixture, water and 1 N HCl were added to acidify the reaction at pH 2.5, and the mixture was allowed to stir for 15 min. After adjustment to pH 6 with 20% NaOH (aq), chloroform was used for extraction. The extraction was repeated at pH 6.5 and 8.3. The extract at pH 8.3 was concentrated, and dry ether was added. After the mixture was stirred for 2 h in the ice bath, the precipitant was vacuum-dried to yield **8** (300 mg, 61%) as a white powder. ¹H NMR (500 MHz, CDCl_3) δ 5.09 (d, $J = 4.6$ Hz, 1H), 4.71 (dd, $J = 10.3, 2.2$ Hz, 1H), 4.42 (d, $J = 7.3$ Hz, 1H), 4.32 (dd, $J = 4.3, 1.9$ Hz, 1H), 4.07 (dq, $J = 12.3, 6.2$ Hz, 1H), 3.64 (d, $J = 7.4$ Hz, 1H), 3.49 (tdd, $J = 11.2, 6.4, 4.6$ Hz, 1H), 3.44 (d, $J = 1.7$ Hz, 1H), 3.38 (s, 1H), 3.33 (s, 3H), 3.22 (dd, $J = 10.2, 7.4$ Hz, 1H), 3.08–2.99 (m, 3H), 2.92 (s, 1H), 2.76 (qd, $J = 7.4, 4.8$ Hz, 1H), 2.59–2.53 (m, 1H), 2.43 (ddd, $J = 12.3, 10.4, 3.8$ Hz, 1H), 2.34 (d, $J = 15.2$ Hz, 1H), 2.27 (s, 6H), 2.26–2.23 (m, 1H), 2.17 (d, $J = 10.5$ Hz, 1H), 1.96–1.89 (m, 1H), 1.88

(ddd, $J = 14.2, 7.6, 2.3$ Hz, 1H), 1.82 (t, $J = 11.3$ Hz, 1H), 1.73 (d, $J = 14.3$ Hz, 2H), 1.68–1.62 (m, 1H), 1.57 (dd, $J = 15.2, 5.0$ Hz, 1H), 1.52–1.42 (m, 1H), 1.36 (dd, $J = 14.9, 7.7$ Hz, 1H), 1.31 (d, $J = 6.2$ Hz, 3H), 1.28 (s, 3H), 1.23 (s, 3H), 1.21 (d, $J = 6.1$ Hz, 4H), 1.19 (d, $J = 7.5$ Hz, 4H), 1.13 (d, $J = 6.5$ Hz, 3H), 1.07 (s, 3H), 1.04 (d, $J = 7.5$ Hz, 3H), 0.92 (d, $J = 6.9$ Hz, 3H), 0.88 (t, $J = 7.4$ Hz, 4H). ^{13}C NMR (500 MHz, CDCl_3) δ 178.95, 103.10, 94.93, 83.43, 78.28, 78.04, 78.01, 73.93, 73.88, 73.16, 73.08, 70.97, 68.87, 65.92, 65.63, 57.47, 56.93, 49.58, 45.50, 42.33, 40.49, 34.87, 30.00, 28.83, 27.58, 22.04, 21.73, 21.51, 21.12, 18.40, 16.24, 15.04, 14.09, 11.28, 9.24. ESI mass spectrum: calcd (MH^+) 735.5; found 735.6.

N9-Propylazithromycin, 9. 9-Deoxy-9a-aza-homoerythromycin A 8 (204 μmol , 150 mg) and propionaldehyde (1021 μmol , 59 mg) were dissolved in DMF (1.5 mL). Acetic acid (2041 μmol , 123 mg) and sodium cyanoborohydride (306 μmol , 19 mg) were added to the reaction mixture. The mixture was stirred for 7 h at 70 °C. The crude mixture was diluted into CH_2Cl_2 and was washed three times with saturated NaHCO_3 (aq) and was dried over Na_2SO_4 . After evaporation of the solvent, the resulting product was purified by flash chromatography, eluting with a step gradient ranging from 3% to 10% $\text{MeOH}/\text{CH}_2\text{Cl}_2$ containing 0.1% NH_4OH (aq) to yield 9 (38 mg, 24%) as a white powder. ^1H NMR (500 MHz, CDCl_3) δ 5.05 (d, $J = 4.5$ Hz, 1H), 4.70 (dd, $J = 9.7, 2.1$ Hz, 1H), 4.43 (d, $J = 7.3$ Hz, 1H), 4.20 (dd, $J = 5.3, 2.3$ Hz, 1H), 4.12 (s, 1H), 4.07 (dt, $J = 15.3, 6.1$ Hz, 1H), 3.76 (s, 1H), 3.64 (d, $J = 6.9$ Hz, 1H), 3.54–3.45 (m, 1H), 3.38 (s, 1H), 3.32 (s, 3H), 3.23 (dd, $J = 10.1, 7.3$ Hz, 1H), 3.02 (t, $J = 8.7$ Hz, 1H), 2.86 (td, $J = 12.9, 4.5$ Hz, 1H), 2.81–2.71 (m, 3H), 2.63 (s, 1H), 2.53 (td, $J = 13.0, 4.3$ Hz, 1H), 2.45 (td, $J = 12.2, 3.8$ Hz, 1H), 2.34 (d, $J = 15.2$ Hz, 1H), 2.28 (s, 6H), 2.20 (d, $J = 9.8$ Hz, 1H), 2.09–1.96 (m, 3H), 1.87 (dtd, $J = 22.0, 7.6, 2.6$ Hz, 1H), 1.73 (d, $J = 14.2$ Hz, 1H), 1.65 (dd, $J = 11.0, 1.8$ Hz, 1H), 1.57 (dd, $J = 15.2, 4.9$ Hz, 2H), 1.51–1.38 (m, 3H), 1.37–1.33 (m, 1H), 1.32 (s, 1H), 1.31 (s, 4H), 1.23 (t, $J = 5.1$ Hz, 5H), 1.21 (t, $J = 6.7$ Hz, 7H), 1.13 (d, $J = 6.8$ Hz, 3H), 1.06 (d, $J = 9.1$ Hz, 6H), 0.91 (d, $J = 7.3$ Hz, 3H), 0.88 (d, $J = 7.4$ Hz, 2H), 0.82 (t, $J = 7.3$ Hz, 3H). ^{13}C NMR (500 MHz, CDCl_3) δ 178.23, 133.57, 103.24, 95.67, 95.27, 83.85, 78.61, 78.19, 77.86, 75.04, 74.26, 73.90, 72.98, 71.01, 68.97, 65.77, 65.73, 65.14, 61.83, 52.16, 49.57, 45.04, 42.07, 41.32, 40.50, 35.03, 29.82, 28.91, 28.48, 27.32, 22.54, 21.72, 21.67, 21.49, 20.46, 18.38, 16.57, 15.06, 12.25, 11.45, 9.61. ESI mass spectrum: calcd (MH^+) 777.5; found 777.5.

N9-Allylazithromycin, 10. 9-Deoxy-9a-aza-homoerythromycin A 8 (204 μmol , 150 mg) was mixed with allyl acetate (10 204 μmol , 1021 mg). TEA (539 μmol , 55 mg) and tetrakis(triphenylphosphine)palladium(0) (20 μmol , 24 mg) was added to the reaction mixture at rt under N_2 . The mixture was stirred for 7 h at 80 °C and further stirred for 15 h at rt under N_2 . The crude mixture was diluted into CH_2Cl_2 and was washed three times with saturated NaHCO_3 (aq) and was dried over Na_2SO_4 . After evaporation of the solvent, the resulting product was purified by flash chromatography, eluting with a step gradient ranging from 3% to 10% $\text{MeOH}/\text{CH}_2\text{Cl}_2$ containing 0.1% NH_4OH (aq) to yield 4 (41 mg, 26%) as a white powder. ^1H NMR (500 MHz, CDCl_3) δ 6.00 (dq, $J = 10.0, 6.8$ Hz, 1H), 5.15–5.02 (m, 3H), 4.70 (dd, $J = 10.0, 2.0$ Hz, 1H), 4.43 (d, $J = 7.3$ Hz, 1H), 4.38 (s, 1H), 4.24–4.20 (m, 1H), 4.07 (dq, $J = 12.4, 6.1$ Hz, 1H), 3.75 (s, 1H), 3.64 (d, $J = 6.9$ Hz, 1H), 3.64–3.57 (m, 1H), 3.50 (dd, $J = 9.8, 5.4$ Hz, 1H), 3.41–3.34 (m, 1H), 3.32 (s, 3H), 3.23 (dd, $J = 10.1, 7.4$ Hz, 1H), 3.02 (t, $J = 9.2$ Hz, 2H), 2.79 (dt, $J = 10.8, 7.1$ Hz, 3H), 2.70 (s, 1H), 2.48–2.41 (m, 1H), 2.35 (d, $J = 15.1$ Hz, 1H), 2.27 (s, 6H), 2.18 (d, $J = 10.2$ Hz, 1H), 2.04–1.97 (m, 3H), 1.87 (dq, $J = 15.2, 7.5, 2.5$ Hz, 1H), 1.71 (d, $J = 14.3$ Hz, 1H), 1.67–1.62 (m, 1H), 1.57 (dd, $J = 15.2, 5.0$ Hz, 1H), 1.52–1.42 (m, 1H), 1.31–1.32 (m, 6H), 1.23 (s, 3H), 1.19–1.22 (m, 6H), 1.14 (d, $J = 6.8$ Hz, 3H), 1.07 (s, 3H), 1.06 (d, $J = 7.5$ Hz, 3H), 0.88 (t, $J = 7.5$ Hz, 3H), 0.86 (d, $J = 5.9$ Hz, 3H). ^{13}C NMR (500 MHz, CDCl_3) δ 178.38, 136.45, 117.66, 103.18, 95.21, 83.77, 78.46, 78.20, 77.80, 74.88, 74.36, 74.10, 73.00, 70.99, 68.95, 65.80, 65.75, 61.83, 53.57, 49.58, 45.12, 41.96, 41.52, 40.50, 34.98, 28.87, 27.80, 27.15, 22.19, 21.72, 21.60, 21.50, 18.39, 16.49, 15.01, 11.42, 9.85, 9.54. ESI mass spectrum: calcd (MH^+) 775.5; found 775.4.

N9-Ethylamideazithromycin, 12. 9-Deoxy-9a-aza-homoerythromycin A 8 (88 μmol , 65 mg) was dissolved in toluene (1.8 mL). Ethyl isocyanate (91 μmol , 6 mg) was added to the reaction mixture, and the mixture was stirred for 1 h at rt. After evaporation of the solvent, the crude mixture was diluted into CH_2Cl_2 and was washed three times with saturated NaHCO_3 (aq) and was dried over Na_2SO_4 . The resulting product was purified by flash chromatography, eluting with a step gradient ranging from 3% to 10% $\text{MeOH}/\text{CH}_2\text{Cl}_2$ containing 0.1% NH_4OH (aq) to yield 12 (33 mg, 47%) as a white powder. ^1H NMR (500 MHz, CDCl_3) δ 4.99 (dd, $J = 9.3, 2.7$ Hz, 1H), 4.83 (d, $J = 4.2$ Hz, 1H), 4.66 (s, 1H), 4.45 (d, $J = 7.2$ Hz, 1H), 4.05 (td, $J = 12.7, 6.3$ Hz, 1H), 4.01–3.98 (m, 1H), 3.75 (s, 1H), 3.59 (dd, $J = 9.9, 4.8$ Hz, 1H), 3.49 (d, $J = 4.4$ Hz, 1H), 3.44 (d, $J = 14.3$ Hz, 1H), 3.32 (dd, $J = 10.5, 6.8$ Hz, 1H), 3.27 (s, 3H), 3.24–3.16 (m, 3H), 3.02 (d, $J = 7.3$ Hz, 1H), 2.66 (dt, $J = 12.4, 6.2$ Hz, 1H), 2.59–2.49 (m, 2H), 2.29 (s, 6H), 2.34–2.25 (m, 9H), 2.14 (s, 2H), 1.91 (ddd, $J = 14.1, 7.5, 3.0$ Hz, 2H), 1.70–1.61 (m, 2H), 1.55 (dd, $J = 15.1, 4.9$ Hz, 1H), 1.46 (ddd, $J = 14.4, 9.2, 7.3$ Hz, 1H), 1.30 (d, $J = 6.9$ Hz, 3H), 1.26 (d, $J = 6.1$ Hz, 6H), 1.24–1.20 (m, 9H), 1.13 (s, 2H), 1.11 (t, $J = 7.2$ Hz, 3H), 1.04 (t, $J = 7.0$ Hz, 6H), 0.89 (t, $J = 7.4$ Hz, 3H). ^{13}C NMR (500 MHz, CDCl_3) δ 159.86, 104.64, 96.84, 79.23, 78.23, 77.60, 74.68, 74.59, 74.17, 72.95, 70.84, 69.52, 66.36, 64.77, 49.46, 46.28, 41.36, 40.56, 35.91, 35.15, 29.41, 28.25, 22.46, 21.63, 21.33, 21.23, 17.91, 17.45, 15.46, 15.08, 12.57, 11.57, 10.40. ESI mass spectrum: calcd (MH^+) 806.5; found 806.6.

C6-Methoxyl-9-Deoxy-9a-aza-homoerythromycin A, 14. Clarithromycin (5.4 mmol, 4 g), 50% hydroxylamine (7 mL), and acetic acid (5 mL) in isopropanol was stirred for 5 days at 40 °C to yield 6-methoxyerythromycin A 9-oxime as a white solid (2.6 g, 64%). C6-Methoxyerythromycin A 9-oxime (3.4 mmol, 2.6 g), toluene-*p*-sulfonyl chloride (6.81 mmol, 1.3 g), and pyridine (6.81 mmol, 0.5 g) in THF was stirred for 20 h at 40 °C to yield C6-methoxyerythromycin A 9,11-imino ether (2 g, 80%). C6-Methoxyerythromycin A 9,11-imino ether (2.7 mmol, 2 g) in MeOH was reduced by adding acetic acid and sodium borohydride (18.8 mmol, 0.7 g) to yield 14 as a white powder (460 mg, 23%). ^1H NMR (500 MHz, CDCl_3) δ 4.95 (d, $J = 4.0$ Hz, 1H), 4.86 (dd, $J = 10.8, 2.0$ Hz, 1H), 4.47 (d, $J = 7.3$ Hz, 1H), 4.08–3.98 (m, 2H), 4.00 (dd, $J = 7.2, 1.6$ Hz, 1H), 3.82 (d, $J = 6.4$ Hz, 1H), 3.69–3.58 (m, 1H), 3.51 (dd, $J = 9.8, 5.4$ Hz, 2H), 3.35 (s, 3H), 3.32 (s, 3H), 3.18 (dd, $J = 10.3, 7.3$ Hz, 2H), 3.07–2.98 (m, 2H), 2.86 (dt, $J = 14.8, 7.5$ Hz, 1H), 2.76 (dd, $J = 13.1, 6.5$ Hz, 1H), 2.45–2.38 (m, 1H), 2.34 (d, $J = 15.1$ Hz, 1H), 2.27 (s, 6H), 2.22 (d, $J = 10.7$ Hz, 1H), 2.11 (t, $J = 10.5$ Hz, 1H), 1.92–1.82 (m, 3H), 1.70–1.61 (m, 3H), 1.58 (dd, $J = 9.0, 5.6$ Hz, 1H), 1.50 (ddd, $J = 14.2, 10.9, 7.2$ Hz, 1H), 1.38–1.34 (m, 3H), 1.33–1.28 (m, 1H), 1.30 (d, $J = 6.2$ Hz, 3H), 1.25 (s, 3H), 1.24–1.19 (m, 9H), 1.12 (t, $J = 8.5$ Hz, 1H), 1.07 (s, 3H), 1.06 (d, $J = 7.6$ Hz, 2H), 1.04–1.01 (m, 1H), 0.99 (d, $J = 7.0$ Hz, 2H), 0.88 (t, $J = 7.3$ Hz, 3H). ^{13}C NMR (500 MHz, CDCl_3) δ 177.62, 102.61, 96.05, 79.91, 79.16, 77.99, 73.77, 72.96, 72.74, 71.04, 68.85, 66.14, 65.71, 58.21, 57.23, 51.82, 49.55, 45.30, 40.46, 35.08, 29.83, 28.70, 28.05, 22.01, 21.65, 21.60, 20.90, 20.40, 18.75, 16.27, 16.03, 12.85, 11.06, 9.35. ESI mass spectrum: calcd (MH^+) 749.5; found 749.5.

C6-Alloxy-9-deoxy-9a-aza-9a-homoerythromycin A, 21. Erythromycin A 9-oxime 1a (6.7 mmol, 5 g), pyridine hydrochloride (10 mmol, 1.2 g), and cyclohexane, diethyl ketal (16.7 mmol, 2.9 g) in acetonitrile were stirred for 16 h under N_2 to yield erythromycin A 9-(*O*-ethoxycyclohexyl)oxime. The oxime (6.2 mmol, 5.4 g), pyridine hydrochloride (9.3 mmol, 1.1 g), and hexamethyldisilazane (25 mmol, 5.2 g) in acetonitrile were stirred for 2 h to yield 2',4'-*O*-bis(TMS) erythromycin A 9-(1-(1-ethoxy)cyclohexyl)oxime (5.8 g, 92%). The protected oxime (2 mmol, 2 g), allyl *tert*-butylcarbonate (2.4 mmol, 0.4 g), $\text{Pd}_2(\text{dba})_3$ (29.6 μmol , 37 mg), and dppb (39.2 μmol , 17 mg) in THF was refluxed for 3 h under N_2 . After reflux, the protection groups were removed by acetic acid (5.6 mL) in acetonitrile (20 mL) and H_2O (4 mL) to yield C6-alloxyerythromycin A 9-oxime (1.2 g, 80%).

C6-Alloxyerythromycin A 9-oxime (1.14 mmol, 900 mg), toluene-*p*-sulfonyl chloride (1.71 mmol, 326 mg), and pyridine (2.28 mmol, 180 mg) in THF were stirred for 21 h at 45 °C to yield imino ether product (590 mg, 67%). C6-Alloxyerythromycin A 9, 11-imino ether (713 μ mol, 550 mg) in MeOH was reduced by adding acetic acid and sodium cyanoborohydride (3.6 mmol, 223 mg) to yield **21** as a white powder (240 mg, 44%). ¹H NMR (500 MHz, CDCl₃) δ 6.03 (ddd, *J* = 22.6, 10.6, 5.4 Hz, 1H), 5.25 (dd, *J* = 17.3, 1.8 Hz, 1H), 5.10 (dd, *J* = 10.5, 1.7 Hz, 1H), 5.04 (dd, *J* = 11.0, 2.1 Hz, 1H), 4.86 (d, *J* = 4.5 Hz, 1H), 4.32 (d, *J* = 7.2 Hz, 1H), 4.15 (dd, *J* = 9.4, 1.7 Hz, 1H), 4.05–3.95 (m, 2H), 3.90 (dd, *J* = 12.2, 5.4 Hz, 2H), 3.72 (d, *J* = 8.3 Hz, 1H), 3.47 (ddd, *J* = 10.9, 6.2, 1.9 Hz, 1H), 3.40 (d, *J* = 2.6 Hz, 1H), 3.35–3.27 (m, 3H), 3.16 (dt, *J* = 11.8, 5.8 Hz, 2H), 3.00 (t, *J* = 9.7 Hz, 1H), 2.90 (s, 1H), 2.86–2.81 (m, 2H), 2.44 (ddd, *J* = 12.4, 10.3, 3.8 Hz, 1H), 2.35 (d, *J* = 15.0 Hz, 1H), 2.32–2.23 (m, 2H), 2.27 (s, 6H), 2.21–2.17 (m, 1H), 2.09–1.98 (m, 3H), 1.92 (dtd, *J* = 12.7, 7.4, 5.2 Hz, 2H), 1.67–1.63 (m, 1H), 1.59–1.52 (m, 2H), 1.52–1.45 (m, 2H), 1.39 (s, 3H), 1.29 (d, *J* = 6.2 Hz, 3H), 1.26–1.21 (m, 12H), 1.15 (d, *J* = 7.4 Hz, 3H), 1.09 (s, 3H), 1.03 (d, *J* = 6.4 Hz, 3H), 0.87–0.83 (m, 6H). ¹³C NMR (500 MHz, CDCl₃) δ 174.74, 136.79, 115.08, 103.96, 103.34, 97.91, 92.09, 83.17, 82.65, 81.03, 78.27, 77.64, 73.60, 72.68, 71.25, 69.03, 67.93, 65.77, 65.70, 63.32, 51.23, 49.79, 49.54, 45.85, 40.83, 40.48, 39.58, 35.88, 29.84, 28.75, 26.78, 25.32, 21.65, 21.51, 21.25, 19.79, 18.61, 17.27, 16.27, 15.25, 10.86, 9.74. ESI mass spectrum: calcd (MH⁺) 775.5; found 775.7.

Minimum Inhibitory Concentration (MIC) Analysis of *Bacillus subtilis*. LB medium was used to grow *B. subtilis* cultures. A standard 2-fold serial dilution method in a 96-well plate was used to determine the MIC of each antibiotic compound against *B. subtilis*. *B. subtilis* cultures were incubated in the presence of antibiotics at 30 °C for 16–18 h, and the optical density was monitored at 490 nm.

***Toxoplasma gondii* Replication Assay.** Tachyzoites of *T. gondii* strains RH Δ hxgp^{rt} YFP, GFP, or clin^R-4 were harvested from cultured human foreskin fibroblast (HFF) monolayers grown in 25 cm² T-flasks and inoculated onto confluent HFF cells in multiwell culture plates (six-well, 2 \times 10⁵ tachyzoites/9.6 cm² well; 12-well, 2 \times 10⁴ parasite tachyzoites/3.8 cm² well; and 96-well, 8 \times 10³ parasite tachyzoites/0.32 cm² well). For the “0 h” protocol, the test compound was added to the appropriate wells simultaneously with parasites, and the cultures were incubated for 48 h before analysis or use in the second infection cycle. In the “6 h” protocol, parasites were preincubated with HFF cells for 6 h. Thereafter, the supernatant containing uninfected parasites was replaced with fresh medium containing the appropriate antibiotic dose, and cultures were incubated for 42 h before analysis or use in the second infection cycle. In experiments involving a second infection cycle, purified extracellular tachyzoites harvested at the end of the first cycle were inoculated into fresh cultures without antibiotic compounds. Infected cultures were incubated at 37 °C, 5% CO₂ in DMEM (Dulbecco’s modified Eagle medium) buffer supplemented with 1% PS (penicillin–streptomycin) and 10% fetal bovine serum. In all experiments, the reported data are from experiments performed at least in triplicate.

Monitoring Parasite Growth by Fluorescence. Tachyzoites from the RH Δ hxgp^{rt} of *T. gondii* with the YFP gene were inoculated and cultured in 96-well plates in the same manner as above. However, parasite growth was monitored in a SpectraMax Gemini EM fluorescent plate reader (Sunnyvale, CA). Both excitation (510 nm) and emission (540 nm) were read from the bottom.

Cytotoxicity Assay. HFF cell cytotoxicity was determined by a standard MTS (3-(4,5-dimethylthiazol-2-yl)-5-(3-carboxymethoxyphenyl)-2H-tetrazolium) assay (CellTiter 96 Aqueous One Solution Assay; Promega). Low passage HFF cells (2 \times 10³ cells/well) were seeded into the 96-well culture plates and incubated for 24 h at 37 °C. Then the HFF cells were exposed to varying concentrations of macrolides for 2 days. After incubation, the macrolide treated medium was

aspirated, and 100 μ L DMEM was added followed by 20 μ L of MTS. The plates were incubated for 4 h at 37 °C, and the optical density was measured at 490 nm. CC₅₀ was calculated as the dose of each macrolide that reduced cell viability by 50%.

Parasite Cell Division Assay. HFF cells were placed on glass coverslips in 12-well plates, and tachyzoites of the RH Δ hxgp^{rt} of *T. gondii* harboring a GFP gene were inoculated and cultured as above. The coverslips were mounted onto glass microscope slides, and the number of parasites in individual parasitophorous vacuole was counted by fluorescence microscopy (Olympus BX60 microscope, 100 \times , NA 1.4/0.9 objective).

RT-PCR Assay. Tachyzoites of the *T. gondii* strain RH Δ hxgp^{rt} GFP and Clin^R-4 were cultured in six-well plates as above and then collected by centrifugation at 2000 rpm for 10 min. The total DNA was extracted using the DNeasy kit (Qiagen, Hilden, Germany) and stored at –20 °C until use. PCR primers 5'-CCAATATGTAACATTTTAGTTCAG-TATCA-3' (forward) and 5'-GGTCAGTAATAACTTGGAAATATC-CTTCTAC-3' (reverse) yielded a 130 bp nucleotide product from the apicoplast genome (*ycf24*), and primers 5'-AACAACTGCGGAGCC-TAAGG-3' (forward) and 5'-TGCACCTCGAAGACACCTGATG-3' (reverse) yielded an 89 bp fragment of the nuclear uracil phosphoribosyl transferase gene (*UPRT*). RT-PCR was performed using the 7900HT fast real-time PCR system (Applied Biosystems) with the following amplification conditions: 1 cycle at 94 °C for 20 s, 40 cycles of 94 °C for 3 s, and 60 °C for 30 s.

■ ASSOCIATED CONTENT

Supporting Information. Multiple sequence alignment (Table S1); synthesis details of compounds **5–7**, **11**, **13**, **15–20**, and **22–31**; and molecular modeling. This material is available free of charge via the Internet at <http://pubs.acs.org>.

■ AUTHOR INFORMATION

Corresponding Author

*Phone: (650) 723-6538. Fax: (650) 725-7294. E-mail: khosla@stanford.edu

■ ACKNOWLEDGMENT

This research was supported by grants from the NIH (Grant R01 GM 087934 to C.K., Grant R01 AL 41014 to J.C.B., and Grant 5U54MH074404, Hugh Rosen, Principal Investigator, which supported the work of J.Y.C. and W.R.R.).

■ ABBREVIATIONS USED

AZ, azithromycin; MIC, minimum inhibitory concentration; IC₅₀, half-maximal inhibitory concentration; CC₅₀, half-maximal cytotoxic concentration; YFP, yellow fluorescent protein; GFP, green fluorescent protein; RT-PCR, real time polymerase chain reaction

■ REFERENCES

- (1) Jones, J. L.; Lopez, A.; Wilson, M.; Schulkin, J.; Gibbs, R. Congenital toxoplasmosis: a review. *Obstet. Gynecol. Surv.* **2001**, *56*, 296–305.
- (2) Luft, B. J.; Remington, J. S. Toxoplasmic encephalitis in AIDS. *Clin. Infect. Dis.* **1992**, *15*, 211–222.
- (3) Kasper, L. H.; Buzoni-Gatel, D. Some opportunistic parasitic infections in AIDS: Candidiasis, pneumocystosis, cryptosporidiosis, toxoplasmosis. *Parasitol. Today* **1998**, *14*, 150–156.

- (4) Fichera, M. E.; Roos, D. S. A plastid organelle as a drug target in apicomplexan parasites. *Nature* **1997**, *390*, 407–409.
- (5) Baird, J. K. Drug therapy: effectiveness of antimalarial drugs. *N. Engl. J. Med.* **2005**, *352*, 1565–1577.
- (6) White, N. J. The treatment of malaria. *N. Engl. J. Med.* **1996**, *335*, 800–806.
- (7) Lell, B.; Kremsner, P. G. Clindamycin as an antimalarial drug: review of clinical trials. *Antimicrob. Agents Chemother.* **2002**, *46*, 2315–2320.
- (8) Pfefferkorn, E. R.; Borotz, S. E. Comparison of mutants of *Toxoplasma gondii* selected for resistance to azithromycin, spiramycin, or clindamycin. *Antimicrob. Agents Chemother.* **1994**, *38*, 31–37.
- (9) Araujo, F. G.; Shepard, R. M.; Remington, J. S. In vivo activity of the macrolide antibiotics azithromycin, roxithromycin and spiramycin against *Toxoplasma gondii*. *Eur. J. Clin. Microbiol.* **1991**, *10*, 519–524.
- (10) Dunne, M. W.; Singh, N.; Shukla, M.; Valecha, N.; Bhattacharyya, P. C.; Dev, V.; Patel, K.; Mohapatra, M. K.; Lakhani, J.; Benner, R.; Lele, C.; Patki, K. A multicenter study of azithromycin, alone and in combination with chloroquine, for the treatment of acute uncomplicated *Plasmodium falciparum* malaria in India. *J. Infect. Dis.* **2005**, *191*, 1582–1588.
- (11) Gingras, B. A.; Jensen, J. B. Antimalarial activity of azithromycin and erythromycin against *Plasmodium berghei*. *Am. J. Trop. Med. Hyg.* **1993**, *49*, 101–105.
- (12) Heppner, D. G.; Walsh, D. S.; Uthaimongkol, N.; Tang, D. B.; Tulyayon, S.; Permpanich, B.; Wimonwattawatee, T.; Chuanak, N.; Laoboonchai, A.; Sookto, P.; Brewer, T. G.; McDaniel, P.; Eamsila, C.; Yongvanitchit, K.; Uhl, K.; Kyle, D. E.; Keep, L. W.; Miller, R. E.; Wongsrichanalai, C. Randomized, controlled, double-blind trial of daily oral azithromycin in adults for the prophylaxis of *Plasmodium vivax* malaria in western Thailand. *Am. J. Trop. Med. Hyg.* **2005**, *73*, 842–849.
- (13) Girard, A. E.; Girard, D.; English, A. R.; Gootz, T. D.; Cimochoowski, C. R.; Faiella, J. A.; Haskell, S. L.; Retsema, J. A. Pharmacokinetic and in vivo studies with azithromycin (CP-62,993), a new macrolide with an extended half-life and excellent tissue distribution. *Antimicrob. Agents Chemother.* **1987**, *31*, 1948–1954.
- (14) Gray, R. H.; Wabwire-Mangen, F.; Kigozi, G.; Sewankambo, N. K.; Serwadda, D.; Moulton, L. H.; Quinn, T. C.; O'Brien, K. L.; Meehan, M.; Abramowsky, C.; Robb, M.; Wawer, M. J. Randomized trial of presumptive sexually transmitted disease therapy during pregnancy in Rakai, Uganda. *Am. J. Obstet. Gynecol.* **2001**, *185*, 1209–1217.
- (15) Wawer, M. J.; Sewankambo, N. K.; Serwadda, D.; Quinn, T. C.; Paxton, L. A.; Kiwanuka, N.; Wabwire-Mangen, F.; Li, C. J.; Lutalo, T.; Nalugoda, F.; Gaydos, C. A.; Moulton, L. H.; Meehan, M. O.; Ahmed, S.; Gray, R. H.; Grp, R. P. S. Control of sexually transmitted diseases for AIDS prevention in Uganda: a randomised community trial. *Lancet* **1999**, *353*, 525–535.
- (16) Schluenzen, F.; Tocilj, A.; Zarivach, R.; Harms, J.; Gluehmann, M.; Janell, D.; Bashan, A.; Bartels, H.; Agmon, I.; Franceschi, F.; Yonath, A. Structure of functionally activated small ribosomal subunit at 3.3 angstrom resolution. *Cell* **2000**, *102*, 615–623.
- (17) Wimberly, B. T.; Brodersen, D. E.; Clemons, W. M.; Morgan-Warren, R. J.; Carter, A. P.; Vornrhein, C.; Hartsch, T.; Ramakrishnan, V. Structure of the 30S ribosomal subunit. *Nature* **2000**, *407*, 327–339.
- (18) Harms, J.; Schluenzen, F.; Zarivach, R.; Bashan, A.; Gat, S.; Agmon, I.; Bartels, H.; Franceschi, F.; Yonath, A. High resolution structure of the large ribosomal subunit from a mesophilic eubacterium. *Cell* **2001**, *107*, 679–688.
- (19) Ban, N.; Nissen, P.; Hansen, J.; Moore, P. B.; Steitz, T. A. The complete atomic structure of the large ribosomal subunit at 2.4 angstrom resolution. *Science* **2000**, *289*, 905–920.
- (20) Carter, A. P.; Clemons, W. M.; Brodersen, D. E.; Morgan-Warren, R. J.; Wimberly, B. T.; Ramakrishnan, V. Functional insights from the structure of the 30S ribosomal subunit and its interactions with antibiotics. *Nature* **2000**, *407*, 340–348.
- (21) Schlunzen, F.; Zarivach, R.; Harms, J.; Bashan, A.; Tocilj, A.; Albrecht, R.; Yonath, A.; Franceschi, F. Structural basis for the interaction of antibiotics with the peptidyl transferase centre in eubacteria. *Nature* **2001**, *413*, 814–821.
- (22) Schlunzen, F.; Harms, J. M.; Franceschi, F.; Hansen, H. A. S.; Bartels, H.; Zarivach, R.; Yonath, A. Structural basis for the antibiotic activity of ketolides and azalides. *Structure* **2003**, *11*, 329–338.
- (23) Hansen, J. L.; Ippolito, J. A.; Ban, N.; Nissen, P.; Moore, P. B.; Steitz, T. A. The structures of four macrolide antibiotics bound to the large ribosomal subunit. *Mol. Cell* **2002**, *10*, 117–128.
- (24) Hansen, J. L.; Moore, P. B.; Steitz, T. A. Structures of five antibiotics bound at the peptidyl transferase center of the large ribosomal subunit. *J. Mol. Biol.* **2003**, *330*, 1061–1075.
- (25) Auerbach, T.; Bashan, A.; Yonath, A. Ribosomal antibiotics: structural basis for resistance, synergism and selectivity. *Trends Biotechnol.* **2004**, *22*, 570–576.
- (26) Ma, Z. K.; Clark, R. F.; Brazzale, A.; Wang, S. Y.; Rupp, M. J.; Li, L. P.; Griesgraber, G.; Zhang, S. M.; Yong, H.; Phan, L. T.; Nemoto, P. A.; Chu, D. T. W.; Plattner, J. J.; Zhang, X. L.; Zhong, P.; Cao, Z. S.; Nilius, A. M.; Shortridge, V. D.; Flamm, R.; Mitten, M.; Meullbroek, J.; Ewing, P.; Alder, J.; Or, Y. S. Novel erythromycin derivatives with aryl groups tethered to the C-6 position are potent protein synthesis inhibitors and active against multidrug-resistant respiratory pathogens. *J. Med. Chem.* **2001**, *44*, 4137–4156.
- (27) Berisio, R.; Schluenzen, F.; Harms, J.; Bashan, A.; Auerbach, T.; Baram, D.; Yonath, A. Structural insight into the role of the ribosomal tunnel in cellular regulation. *Nat. Struct. Biol.* **2003**, *10*, 366–370.
- (28) Chantot, J. F.; Bryskier, A.; Gasc, J. C. Antibacterial activity of roxithromycin—a laboratory evaluation. *J. Antibiot.* **1986**, *39*, 660–668.
- (29) Gasc, J. C.; Dambrieres, S. G.; Lutz, A.; Chantot, J. F. New ether oxime derivatives of erythromycin A: a structure–activity relationship study. *J. Antibiot.* **1991**, *44*, 313–330.
- (30) Kobrehel, G. Z.; Djokic, S. 11-Methyl-11-aza-4-0-cladinosyl-6-0-desosaminyl-15-ethyl-7,13,14-trihydroxy-3,5,7,9,12,14-hexamethyl-oxacyclopentadecane-2-one and Derivatives Thereof. U.S. Patent 4517359, 1985; PLIVA.
- (31) Bright, G. M. N-Methyl 11-aza-10-deoxy-10-dihydro-erythromycin A, Intermediates Thereof. U.S. Patent 4474768, 1984; Pfizer Inc.
- (32) Djokic, S.; Kobrehel, G.; Lazarevski, G.; Lopotar, N.; Tamburasev, Z.; Kamenar, B.; Nagl, A.; Vickovic, I. Erythromycin series. Part 11. Ring expansion of erythromycin A oxime by the beckmann rearrangement. *J. Chem. Soc., Perkin Trans. 1* **1986**, 1881–1890.
- (33) Djokic, S.; Kobrehel, G.; Lopotar, N.; Kamenar, B.; Nagl, A.; Mrvos, D. Erythromycin series. Part 13. Synthesis and structure elucidation of 10-dihydro-10-deoxy-11-methyl-11-azaerythromycin-A. *J. Chem. Res.* **1988**, *5*, 152–153.
- (34) Yang, B. W. V.; Goldsmith, M.; Rizzi, J. P. A novel product from beckmann rearrangement of erythromycin A 9(E)oxime. *Tetrahedron Lett.* **1994**, *35*, 3025–3028.
- (35) Kirst, H. A.; Wind, J. A.; Leeds, J. P.; Willard, K. E.; Debono, M.; Bonjouklian, R.; Greene, J. M.; Sullivan, K. A.; Paschal, J. W.; Deeter, J. B.; Jones, N. D.; Ott, J. L.; Feltyduckworth, A. M.; Counter, F. T. Synthesis and structure–activity-relationships of new 9-N-alkyl derivatives of 9(S)-erythromycylamine. *J. Med. Chem.* **1990**, *33*, 3086–3094.
- (36) Gubbels, M. J.; Li, C.; Striepen, B. High-throughput growth assay for *Toxoplasma gondii* using yellow fluorescent protein. *Antimicrob. Agents Chemother.* **2003**, *47*, 309–316.
- (37) Djokic, S.; Kobrehel, G.; Lazarevski, G. Erythromycin series. 12. Antibacterial in vitro evaluation of 10-dihydro-10-deoxy-11-azaerythromycin A: synthesis and structure–activity relationship of its acyl derivatives. *J. Antibiot.* **1987**, *40*, 1006–1015.
- (38) Bright, G. M.; Nagel, A. A.; Bordner, J.; Desai, K. A.; Dibrino, J. N.; Nowakowska, J.; Vincent, L.; Watrous, R. M.; Scivolino, F. C.; English, A. R.; Retsema, J. A.; Anderson, M. R.; Brennan, L. A.; Borovoy, R. J.; Cimochoowski, C. R.; Faiella, J. A.; Girard, A. E.; Girard, D.; Herbert, C.; Manousos, M.; Mason, R. Synthesis, in vitro and in vivo activity of novel 9-deoxy-9a-aza-9a-homoerythromycin derivatives—a new class of macrolide antibiotics, the azalides. *J. Antibiot.* **1988**, *41*, 1029–1047.
- (39) Kujundzic, N. S.; Kobrehel, G.; Kelneric, Z. 9a-N-(N'-Carbamoyl) and 9a-N-(N'-Thiocarbamoyl) Derivatives of 9-Deoxy-9a-aza-9a-homoerythromycin A. EP 0657464, 1996.

(40) Pfefferkorn, E. R.; Nothnagel, R. F.; Borotz, S. E. Parasitocidal effect of clindamycin on *Toxoplasma gondii* grown in cultured-cells and selection of a drug-resistant mutant. *Antimicrob. Agents Chemother.* **1992**, *36*, 1091–1096.

(41) Fichera, M. E.; Bhopale, M. K.; Roos, D. S. In vitro assays elucidate peculiar kinetics of clindamycin action against *Toxoplasma gondii*. *Antimicrob. Agents Chemother.* **1995**, *39*, 1530–1537.

(42) McCabe, R. E.; Oster, S. Current recommendations and future-prospects in the treatment of toxoplasmosis. *Drugs* **1989**, *38*, 973–987.

(43) Zhao, Q.; Zhang, M.; Hong, L. X.; Zhou, K. F.; Lin, Y. G. Evaluation of drug effects on *Toxoplasma gondii* nuclear and plastid DNA replication using real-time PCR. *Parasitol. Res.* **2010**, *106*, 1257–1262.

(44) Camps, M.; Arrizabalaga, G.; Boothroyd, J. An rRNA mutation identifies the apicoplast as the target for clindamycin in *Toxoplasma gondii*. *Mol. Microbiol.* **2002**, *43*, 1309–1318.

(45) Gregory, S. T.; Dahlberg, A. E. Erythromycin resistance mutations in ribosomal proteins L22 and L4 perturb the higher order structure of 23 S ribosomal RNA. *J. Mol. Biol.* **1999**, *289*, 827–834.

(46) Peric, M.; Bozdogan, B.; Jacobs, M. R.; Appelbaum, P. C. Effects of an efflux mechanism and ribosomal mutations on macrolide susceptibility of *Haemophilus influenzae* clinical isolates. *Antimicrob. Agents Chemother.* **2003**, *47*, 1017–1022.

(47) Prunier, A. L.; Trong, H. N.; Tande, D.; Segond, C.; Leclercq, R. Mutation of L4 ribosomal protein conferring unusual macrolide resistance in two independent clinical isolates of *Staphylococcus aureus*. *Microb. Drug Resist.* **2005**, *11*, 18–20.

(48) Bogdanovich, T.; Bozdogan, B.; Appelbaum, P. C. Effect of efflux on telithromycin and macrolide susceptibility in *Haemophilus influenzae*. *Antimicrob. Agents Chemother.* **2006**, *50*, 893–898.

(49) Clark, C.; Bozdogan, B.; Peric, M.; Dewasse, B.; Jacobs, M. R.; Appelbaum, P. C. In vitro selection of resistance in *Haemophilus influenzae* by amoxicillin-clavulanate, cefpodoxime, cefprozil, azithromycin, and clarithromycin. *Antimicrob. Agents Chemother.* **2002**, *46*, 2956–2962.

(50) Harms, J. M.; Wilson, D. N.; Schluenzen, F.; Connell, S. R.; Stachelhaus, T.; Zaborowska, Z.; Spahn, C. M. T.; Fucini, P. Translational regulation via L11: molecular switches on the ribosome turned on and off by thiostrepton and micrococin. *Mol. Cell* **2008**, *30*, 26–38.

(51) Bissantz, C.; Kuhn, B.; Stahl, M. A medicinal chemist's guide to molecular interactions. *J. Med. Chem.* **2010**, *53*, 5061–5084.

(52) Compound **30**, which possesses two more extended carbons than **11**, may have favorable interaction with Phe98.

(53) Dynamic calculations were performed with fixed potential except the loop region of L22 (Lys94–Arg108), **11**, and adjacent amino acids and RNA fragments within 4 Å from the loop region. However, significant improvement of the interactions between the two phenyl groups was not observed because of packed environment near the loop region of L22 with fixed rRNA fragments.

(54) Viluksela, M.; Vainio, P. J.; Tuominen, R. K. Cytotoxicity of macrolide antibiotics in a cultured human liver cell line. *J. Antimicrob. Chemother.* **1996**, *38*, 465–473.

(55) Vorbach, H.; Armbruster, C.; Robibaro, B.; Griesmacher, A.; El Menyawi, I.; Daxecker, H.; Raab, M.; Muller, M. M. Endothelial cell compatibility of azithromycin and erythromycin. *J. Antimicrob. Chemother.* **2002**, *49*, 407–409.

(56) Millrose, M.; Kruse, M.; Flick, B.; Stahlmann, R. Effects of macrolides on proinflammatory epitops on endothelial cells in vitro. *Arch. Toxicol.* **2009**, *83*, 469–476.

(57) Bonay, P.; Munro, S.; Fresno, M.; Alarcon, B. Intra-Golgi transport inhibition by megalomicin. *J. Biol. Chem.* **1996**, *271*, 3719–3726.

(58) Bonay, P.; Fresno, M.; Alarcon, B. Megalomicin disrupts lysosomal functions. *J. Cell Sci.* **1997**, *110*, 1839–1849.